An Improved Adaptive Coding and Modulation Scheme With Hybrid Switching Standard for UAV-to-Ground Free Space Optical Communication

Qianwu Zhang, Boyang Liu, Guanwen Chen, Shucheng Zhan, Zhiyu Li, Jing Zhang, Ning Jiang, Bingyao Cao, and Zhengxuan Li

***Abstract*—In this paper, an improved adaptive coding and modulation scheme with hybrid switching standard is proposed for UAV-to-Ground free space optical (FSO) communication to mitigate the degradation of turbulence intensity variation. In order to improve bits efficiency in different turbulence, a channel estimator based on Gated Recurrent Unit (GRU) and a hybrid switching standard based on frame error rate (FER) of LDPC decoding are applied. Simulation results show that the GRU estimator achieves approximately 34.9% improvement in training time compared to the LSTM estimator, without degradation in system performance. Moreover, the hybrid switching standard significantly improves the signal-to-noise ratio (SNR) switching threshold deviation of the ACM scheme from 1.8 dB and 4 dB, which were observed in moderate turbulence conditions, to an average of 0.35 dB. This improvement allows for the effective implementation of the ACM scheme in different turbulence intensities at a relatively small cost, thereby enhancing the communication quality of FSO systems in atmospheric channels characterized by turbulent variations.**

***Index Terms*—UAV, FSO, ACM.**

I. Introduction

FREE space optical (FSO) communication is a wireless method that utilizes laser beams to transmit data through the air instead of optical fibers [1]. In areas where deploying optical fibers is challenging, it is considered as an alternative, cost-effective, and fast-deploying solution. Furthermore, It is regarded as a strong competitor to traditional RF technology due to its advantages such as high-speed transmission data rate, security, absence of bandwidth, and low power consumption [2]. FSO can be used in both space-to-ground and ground-to-ground communications, particularly in last-mile connectivity [3], [4].

Manuscript received 14 September 2023; revised 28 October 2023; accepted 31 October 2023. Date of publication 3 November 2023; date of current version 26 December 2023. This work was supported in part by the National Key Research and Development Program of China under Grant 2021YFB2900800, in part by the Science and Technology Commission of Shanghai Municipality under Grants 22511100902, 22511100502, and 20511102400, and in part by 111 Project under Grant D20031. *(Corresponding author: Qianwu Zhang.)*

Qianwu Zhang, Boyang Liu, Guanwen Chen, Shucheng Zhan, Zhiyu Li, Bingyao Cao, and Zhengxuan Li are with the Key Laboratory of Specialty Optics and Optical Access Networks, Shanghai Institute for Advanced Communication and Data Science, Shanghai University, Shanghai 200072, China (e-mail: zhangqianwu@shu.edu.cn).

Jing Zhang and Ning Jiang are with the School of Information and Communication Engineering, University of Electronic Science and Technology of China, Chengdu 611731, China.

Digital Object Identifier 10.1109/JPHOT.2023.3329648

With the recent popularity of unmanned-aerial-vehicle (UAV), FSO communication for high-speed UAV-to-ground links has gained significant attention due to the increasing demand for transmission rates and bandwidth [5]. Despite its many advantages, there are still challenges and obstacles that need to be overcame in the practical implementation of FSO systems [6], [7], [8]. One of the main causes for performance degradation in FSO systems is atmospheric turbulence, which is caused by the uneven distribution of temperature and pressure in the atmosphere [9], [10]. In practice, atmospheric turbulence induces phase disturbances, resulting in issues such as intensity fluctuations, beam wander, and beam broadening of FSO signals.

The fluctuations of atmospheric turbulence are described by statistical models based on the intensity of turbulence, which are used to assess its impact on the reliability of FSO communication [11], [12]. The widely used models include the Log-Normal distribution, which is suitable for weak turbulence, the Gamma-Gamma distribution for moderate to strong turbulence, and the K-distribution for strong turbulence [13], [14], [15]. These models introduce probability density functions based on the turbulence intensity to describe the effects of turbulence on FSO signals. Among them, the most widely used which is employed in this paper is the Gamma-Gamma model, which utilizes the properties of the Gamma distribution to describe the influence of atmospheric turbulence in vertical links [16]. It effectively describes the impacts of FSO channels from UAV to ground.

The performance of space optical communication systems is deeply influenced by Channel State Information (CSI). Due to the relatively slow variations of channel fading in FSO systems compared to the signal rate, CSI can be accurately estimated by the estimator of receiver. Consequently, to enhance communication reliability and throughput, the transmitter can adjust its transmitting parameters, which has been proven effective in RF communication systems [17], [18].

In existing research of FSO communication system, various types of adaptive transmission systems have been proposed and their feasibility and advantages have been validated. Zhou from Auburn University investigated adaptive power allocation schemes to support high data rats in WDM transmission of RoFSO system [19]. Safi provided an adaptive coding and power control and analyzed the impacts of channel estimation errors in practical FSO systems [20]. Chatzidiamantis raised an adaptive S-PSK modulation schemes in ground FSO systems and offered

efficient utilization of channel capacity [21]. Alshaer from Tanta University provided an adaptive modulation scheme employing SIMO techniques in a satellite-to-ground FSO system in presence of scintillation and beam wander to improve spectrum efficiency [22]. Djordjevic proposed an algorithm to adjust coding and modulation schemes based on CSI while keeping the transmission power constant [23].

In the above literature, the authors proposed different methods of adaptive transmission schemes based on CSI in FSO communication, aiming to improve the reliability and throughput of communication systems. However, they all considered adaptive transmission schemes under the assumption of unchanged turbulence. Because of the presence of turbulence, different turbulence intensities at the same SNR level can also affect communication quality. This implies that while these schemes work well when turbulence remains constant, the situation that adaptive transmission schemes vary for different turbulence strength indicates that turbulence variations can render previously formulated adaptive transmission schemes ineffective or even degrade transmission performance. For instance, applying an adaptive coding and modulation (ACM) scheme designed for weak turbulence in conditions of moderate or strong turbulence would inevitably result in the selected coding and modulation scheme being unable to meet the required BER threshold, thereby leading to a reduction in communication quality or even communication disruption under the same signal-to-noise ratio (SNR). Similarly, employing an ACM scheme tailored for strong turbulence in conditions of moderate or weak turbulence, in the pursuit of achieving an excessively low BER, may lead to the selection of a simpler coding and modulation scheme. However, this would decrease the channel utilization rate, subsequently impacting the bits rate of communication. Therefore, it is necessary to format an improved ACM scheme to adapt to FSO channel with variable turbulence intensity.

In this paper, an improved ACM scheme with hybrid switching standard is proposed for UAV-to-Ground FSO channels to address the problems associated with portability across different turbulence strength, which is validated by simulation. It is observed that the GRU estimator achieves approximately 34.9% improvement in training time compared to the LSTM estimator, without any degradation in system performance. Additionally, a hybrid switching standard based on frame error rate of LDPC decoding is introduced. This significantly improves the SNR switching threshold deviation of the ACM scheme from 1.8 dB and 4 dB to an average of 0.35 dB. This improvement allows for the effective implementation of the ACM scheme in different turbulence intensities at a relatively small cost, thereby enhancing the communication quality of FSO systems in atmospheric channels characterized by turbulent variations.

II. Principle of Proposed Scheme

In this section, we present the system model used in the UAV-to-Ground FSO system and demonstrate the principle of ACM scheme with hybrid switching standard and GRU channel estimator.

A. FSO System Model

The UAV-to-Ground FSO channel model is given by:

$$y = RIx + n, \tag{1}$$

where $\boldsymbol{x}$ is the transmitted optical intensity signal, $\boldsymbol{R}$ is the photodiode responsivity and $\boldsymbol{I}$ is the optical signal after atmosphere turbulence. Besides, $\boldsymbol{y}$ is the received electrical signal and $\boldsymbol{n}$ is the additive white Gaussian noise (AWGN) with zero-mean and variance.

We use Gamma-Gamma distribution to model the random atmospheric variable $\boldsymbol{I}$ whose probability density function is given by:

$$f_{GG}(I) = \frac{2(\alpha\beta)^{\frac{\alpha+\beta}{2}}}{\Gamma(\alpha)\Gamma(\beta)} I^{\frac{\alpha+\beta}{2}-1} K_{\alpha-\beta}\left(2\sqrt{\alpha\beta I}\right); I > 0 \tag{2}$$

where $\Gamma(.)$ is the well-known gamma function, $K(.)$ is the Modified Bessel function of the second kind, and $1/\beta$ and $1/\alpha$ are the variances of the small and large scale eddies, respectively, the α and β are shown as:

$$\alpha = \left[\exp\left(\frac{0.49\sigma_R^2}{\left(1+1.11\sigma_R^{12/5}\right)^{7/6}}\right) - 1\right]^{-1} \tag{3}$$

$$\beta = \left[\exp\left(\frac{0.51\sigma_R^2}{\left(1+0.69\sigma_R^{12/5}\right)^{5/6}}\right) - 1\right]^{-1} \tag{4}$$

$$\sigma_R^2 = 1.23 C_n^2 k^{7/6} z^{11/6}, \tag{5}$$

where σ_R^2 denotes the Rytov variance, $k = 2\pi/\lambda$ is the optical wave number, and z is the propagation distance of FSO links, and C_n^2 is the parameter of index refraction structure. Generally, σ_R^2 is used to differentiate the turbulence intensity. The σ_R^2 below 0.5 is classified as weak turbulence, between 0.5 and 1.6 as moderate turbulence, and values exceeding 1.6 are considered strong turbulence [24].

B. Principle of ACM With Hybrid Switching Standard

The traditional ACM scheme aims to maximize the bits transmitted per symbol interval by utilizing the highest possible coding and modulation order, as long as the bit error rate (BER) remains below an acceptable threshold P [22]. This is achieved by estimating the channel state and instantaneous SNR through the transmission of pilot symbols at the beginning of communication symbols. Through a feedback link (a low data rate radio signal which is assumed to be error-free), the channel state information is sent from the receiver (Rx) to the transmitter (Tx).

The adaptive bit efficiency is defined as the number of bits transmitted per symbol interval after removing redundancy, is given as:

$$R_P^{adp} = \max\left(M_i, Rc_j, P_e\left(h\right) \le P\right) \tag{6}$$

where $\boldsymbol{M_i}$ and $\boldsymbol{R_{cj}}$ denote the modulation and coding order of transmission system separately, $\boldsymbol{P_e}$ is the BER of received signal, and $\boldsymbol{P}$ represents the target BER of communication.

When considering the presence of turbulence in the channel, the traditional ACM scheme formulated based on a fixed turbulence intensity becomes ineffective since different turbulence intensity can affect the BER at the same SNR. Considering the practical limitation that Rx can not estimate the BER without pilot sequences to adjust the ACM scheme in real-time communication. Therefore, we propose a hybrid switching standard based on the FER of LDPC decoding.

The hybrid switching standard is established by determining the lower and upper limits of FER, denoted as $\boldsymbol{f_0}$ and $\boldsymbol{f_1}$, respectively, based on a predefined ACM scheme. At the Rx side, if the FER exceeds $\boldsymbol{f_0}$, the encoding and modulation order is decreased, while if the FER is below $\boldsymbol{f_1}$, the encoding and modulation order is increased. This approach aims to maximize the bit efficiency within the range of $\boldsymbol{f_1} < \boldsymbol{f} < \boldsymbol{f_0}$. The hybrid switching standard we proposed at the Rx side is as follows:

$$\begin{aligned} R_P^{adp} &= \max(M_i, Rc_j, P_e(h) \le P, f_1 < f < f_0) \\ M_i &= 2^i (i = 1, 2), Rc_j \in (1/2, 2/3, 4/5) \end{aligned} \tag{7}$$

where the threshold $\boldsymbol{P}$ in terms of BER represents the forward error correction (FEC) threshold, while the thresholds $\boldsymbol{f_1}$ and $\boldsymbol{f_0}$ for FER are determined based on the ACM scheme with certain redundancy in the presence of moderate turbulence. In the intensity modulation/direct detection (IM/DD) system, the modulation formats considered are OOK and PAM4, while LDPC encoding is used with code rates of {1/2, 2/3, 4/5}.

In a fixed turbulence scenario, the ACM scheme formulated for the given turbulence conditions does not require FER-based corrections. However, under changing turbulence conditions, the ACM scheme, which is no longer suitable for the current channel, can be improved using the hybrid switching standard. This allows the system to adapt to the attenuation caused by turbulence variations and enhance the overall communication quality of the FSO system.

C. Principle of GRU Model

As a type of Recurrent Neural Network (RNN), The Gated Recurrent Unit (GRU) model exhibits advantages in handling sequential signals. In comparison to the conventionally Long Short-Term Memory (LSTM) neural network model, GRU can also be applied for channel estimator. When used to estimate the CSI in the FSO system proposed in this paper, GRU demonstrates shorter training time and requires fewer training resources without compromising performance. The principle of the GRU model is illustrated in the Fig. 2.

GRU can handle time sequences that have correlation with each backward and forward better by reset gate, update gate and candidate hidden state [25]. The functions of each part in GRU are described as:

$$\mathrm{r}_t = \sigma(W_{xr} x_t + W_{hr} h_{t-1} + b_r) \tag{8}$$

$$z_t = \sigma(W_{xz} x_t + W_{hz} h_{t-1} + b_z) \tag{9}$$

$$\widetilde{h}_t = \tanh(W_{xh} x_t + W_{hh}(r_t \circ h_{t-1}) + b_h) \tag{10}$$

$$h_t = (1 - z_t) \circ \widetilde{h}_t + z_t \circ h_{t-1} \tag{11}$$

where $\boldsymbol{r_t}$, $\boldsymbol{z_t}$, and h_t are the outputs of reset gate, update gate and candidate hidden state, respectively. Besides, σ is the sigmoid function, $\boldsymbol{h_t}$, which is updated by $\boldsymbol{z_t}$ and indicates the output value of the block. $\boldsymbol{x_t}$ is the time sequence, and $\circ$ denotes the Hadamard product. $\boldsymbol{W}$ and $\boldsymbol{b}$ are the parameters determined by training of the GRU network.

III. Simulation System Setup

In this paper, the proposed scheme is simulated and validated by Optisystem and MATLAB. The structure of the proposed UAV-to-Ground FSO communication system is illustrated in the Fig. 1. Firstly, at the transmitter, PRBS15 data is encoded using LDPC encoder and modulated by OOK/PAM4 modulator. The signal is modulated by Mach-Zehndar modulator (MZM) at 1550 nm laser provided by continuous wave (CW) laser. The optical signal is transmitted through the UAV-to-Ground FSO channel, which primarily encompasses a 20 km atmospheric channel. Consequently, the channel is affected by both atmospheric-induced signal attenuation and the gamma-gamma distribution representing atmospheric turbulence. These parameters are adjusted by modifying the channel attenuation rate and the atmospheric refractive index parameter, thereby influencing the channel state. At the receiver, an avalanche photodiode (APD) converts the optical signal into an electrical signal. Subsequently, the SNR of the channel is estimated by the GRU channel estimator through Python. After demodulation and decoding of the electrical signal, which is realized by belief propagation algorithm [26], the LDPC decoding FER is analyzed by the FER analyzer. The hyper switching standard, composed of CSI and FER, is used to select the most suitable coding and modulation scheme for the current channel, based on the predefined ACM scheme. This ACM scheme is then transmitted back to the transmitter via a feedback channel (a low data rate radio signal which is assumed to be error-free), which the encoder and modulator at the transmitter adjust the coding and modulation formats according to. Finally, the BER analyzer evaluates the BER of the communication system. The simulation parameters are listed in Table I.

IV. Simulation Results and Discussions

The proposed methods in the ACM scheme for UAV-to-Ground FSO channels are primarily focused on the hybrid switching standard. In the part of channel estimation, a more resource-efficient and faster channel estimator based on GRU is proposed. Additionally, the hybrid switching standard based on FER of LDPC decoding is introduced to address the challenge of poor portability of the ACM scheme across different turbulence conditions. These two methods are necessary in atmospheric channels where turbulence variations are likely to occur. The results and analysis of these improvements are presented as follows.

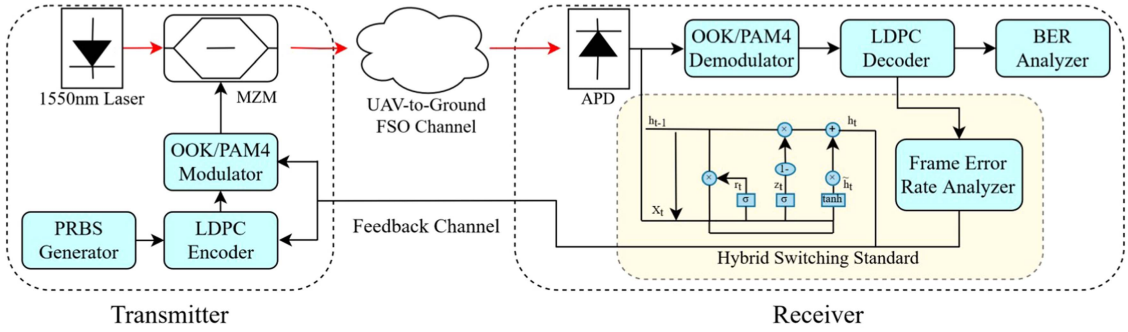

Fig. 1. Structure of the proposed UAV-to-Ground FSO communication system.

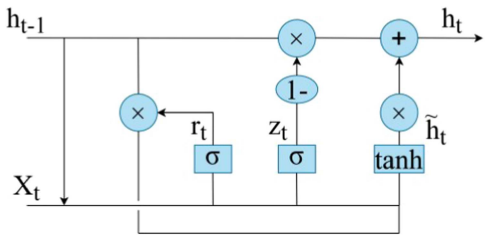

Fig. 2. Principle of GRU.

TABLE I
PARAMETERS USED IN SIMULATION

Parameters	Value
Laser frequency	1550 nm
Link length	20 km
Bit rate	10 Gbps
APD gain	20 dB
APD responsivity	1 A/W
Attenuation coefficient	0.1 dB/km
Zenith angle	60 °
Rytov variance	0.5, 1, 1.6, 3.5
Modulation type	OOK/PAM4
CW laser power	10 dBm
Transmit power	20 dBm
CW laser linewidth	10 MHz
MZM bandwidth	40 GHz
APD bandwidth	48 GHz
APD dark current	10 nA
GRU hidden size	120

A. GRU Channel Estimator

The performance of the GRU estimator model is presented in Fig. 3(a), where the turbulence intensities varies at values of 0.5, 1, 1.6, and 3.5, evaluated by the mean squared error (MSE) metric, which indicates the accuracy of the model's predictions (smaller values indicate better performance). It can be observed that the MSE gradually decreases as the SNR increases, and the overall MSE of the GRU estimator remains consistently below 0.01. Additionally, with increasing turbulence intensity, the MSE exhibits a slight upward trend at the same SNR level. Consequently, the GRU estimator model demonstrates excellent performance in the variable UAV-to-Ground FSO channel.

Moreover, Fig. 3(b) presents the MSE curves of the GRU and LSTM estimators under weak turbulence conditions. As the SNR increases, it can be observed that the MSE of the GRU estimator is comparable to that of the LSTM estimator. As shown in Fig. 3(c), the MSE of both the GRU and LSTM estimators exhibit a decreasing trend as the hidden size increases, particularly at SNR of 20 dB. However, this declining trend becomes less noticeable when the hidden size exceeds 120. Although the MSE of the GRU estimator is consistently slightly higher than that of the LSTM estimator when the hidden size is less than 120, they exhibit parallel MSE behavior when the hidden size surpasses 120. In summary, the GRU estimator model demonstrates similar goodness of fit and prediction accuracy to the LSTM estimator model in the FSO channel.

The Fig. 4(a) provides a comparison of the flops calculation for channel estimation between GRU and LSTM models at different hidden sizes. It is evident that the GRU model requires fewer computational resources during training in comparison to LSTM, and this difference becomes more pronounced as the hidden size increases. These results indicate that GRU is more computationally efficient than LSTM, especially during multiple training iterations, making it a more resource-saving option.

Additionally, as shown in The Fig. 4(b), there is a significant disparity in training time between GRU and LSTM for various hidden sizes. As the hidden size increases, the training time of GRU exhibits a steady rise, whereas the training time of LSTM demonstrates a sharp upward trend. Moreover, the training time of GRU remains consistently below 1.7 hours, while the training time of LSTM exceeds 1.7 hours at a hidden size of 140. Furthermore, at a hidden size of 120, the training time of GRU is 65.1% of the training time of LSTM, despite both models exhibiting similar performance. Hence, based on the observations from Figs. 3 and 4, it can be concluded that the GRU estimator outperforms the LSTM estimator in terms of computational resource consumption and training time, while demonstrating similar performance in UAV-to-Ground FSO channel estimation.

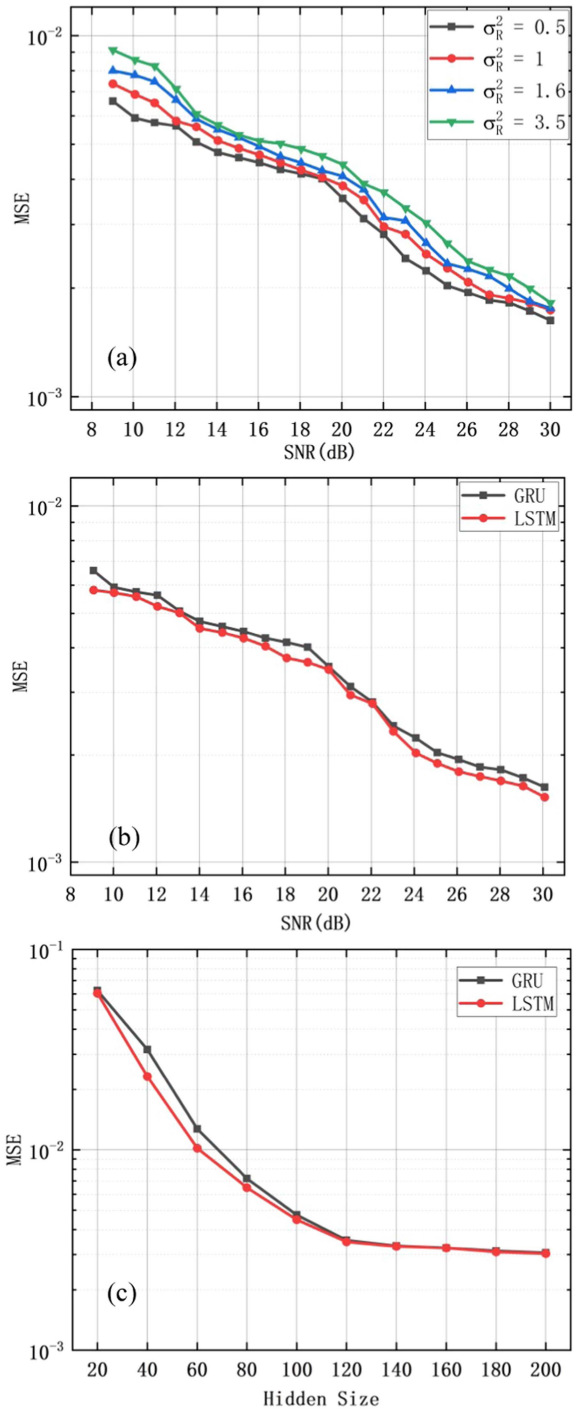

Fig. 3. MSE performance of (a) increasing SNR of GRU estimator at different turbulence intensity (b) GRU and LSTM estimator at weak turbulence (c) different hidden size of GRU and LSTM.

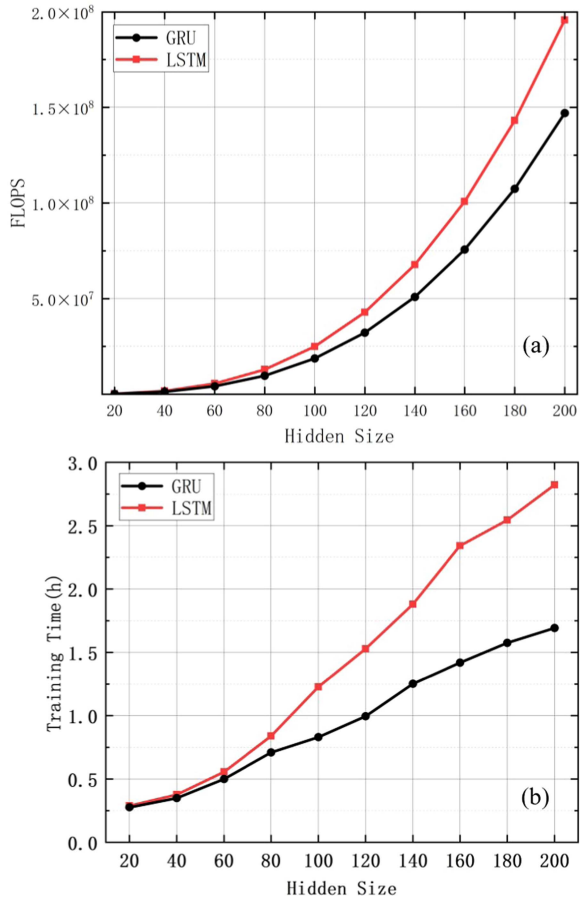

Fig. 4. (a) Training flops (b) training time of GRU and LSTM estimator with different hidden size.

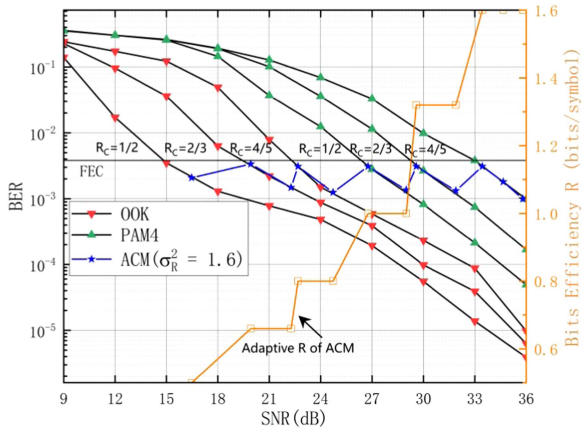

Fig. 5. BER and Bits Efficiency versus SNR with different coding and modulation order under medium turbulence.

B. Hybrid Switching Standard

The results depicted in the Fig. 5 illustrate the performance of conventional adaptive coding and modulation scheme with a single switching standard under medium turbulence intensity. This ACM scheme, as the blue curve shows, enhances the bit efficiency of FSO transmission systems based on the prevailing channel conditions. When the received SNR degrease below the requirements of the current coding and modulation scheme, the scheme progressively reduces the coding and modulation index until the desired SNR is achieved. Conversely, in prefect channel conditions, the ACM scheme will increase the coding and modulation index as long as the BER under FEC threshold. As

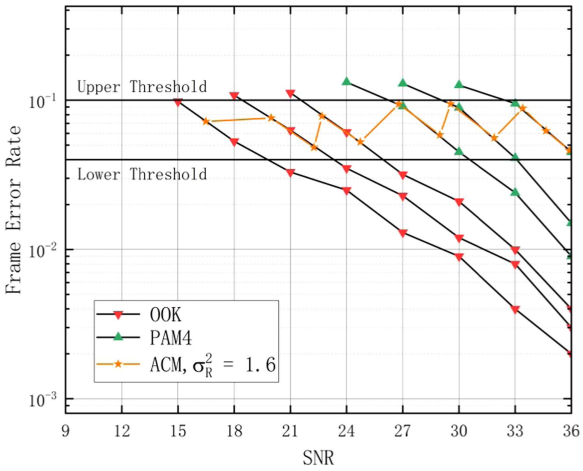

Fig. 6. Frame error rate versus SNR with different coding and modulation order under medium turbulence.

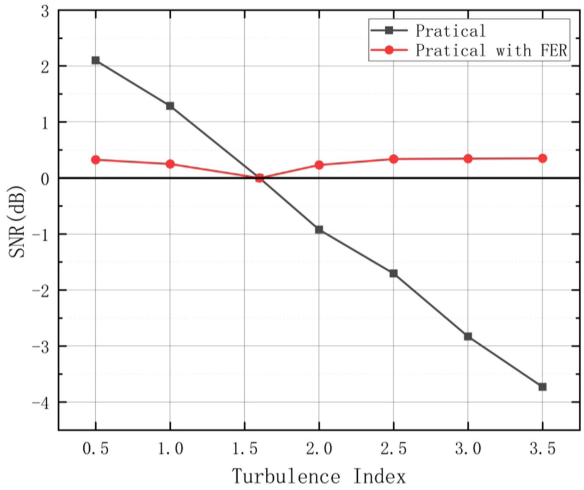

Fig. 7. SNR difference of ACM scheme and ACM scheme with FER switching compared with ideal ACM scheme under different turbulence.

illustrated in the figure, the bit efficiency (R) of the ACM scheme improves from 0.5 bits/symbol (poor channel conditions) to 1.6 bits/symbol (perfect channel conditions), while ensuring that the maximum average BER of the channel is lower than the FEC threshold (3.8×10^{-3}).

To obtain the upper and lower threshold values for LDPC decoding error rate switching in the Hybrid Switching Standard, the LDPC decoding error rate at the receiving end under moderate turbulence is shown in the Fig. 6. It can be observed that with the established ACM scheme, the LDPC decoding error rate remains within a certain range. To allow for some redundancy in the switching scheme, significant margins are reserved at both the maximum and minimum frame error rates. Subsequently, upper and lower thresholds of 1×10^{-1} and 4×10^{-2} were chosen [27].

In other words, when there is a change in turbulence intensity, the LDPC decoding error rate of current communication may surpass the upper or lower thresholds. if the LDPC decoding error rate exceeds the upper threshold, to maintain the current communication quality, the coding and modulation index should be reduced until it meets the threshold. Similarly, if the decoding error rate falls below the lower threshold, the coding and modulation index should be increased until it meets the threshold. This LDPC decoding error rate-based switching criterion, apart from SNR, enables the effective transfer of an ACM scheme obtained under specific turbulence conditions to different turbulence intensities, thus catering to the requirements of rapidly changing turbulent channels.

The ACM scheme from medium turbulence, directly transplanted or adopted with FER switching standard, is transplanted to other turbulence intensity scenarios as illustrated in the Fig. 7. It can be observed that the SNR difference between the directly transplanted ACM scheme and the ideal ACM scheme under the current turbulence is positive when the turbulence is lower than that of the original ACM scheme. This indicates a delay in the coding and modulation index switching, resulting in increased waste in bits efficiency as the SNR decreases. Conversely, when the turbulence intensity is higher than that of the original ACM scheme, the SNR difference is negative. This suggests that the coding and modulation index switching will occur earlier. The larger the absolute value of the interpolation as the turbulence increases, the more likely it is to cause BER to exceed the FEC threshold, leading to communication interruptions.

In contrast, the ACM scheme with FER switching standard, when compared with the ideal scheme under different turbulence conditions, exhibits relatively stable SNR differences, averaging around 0.35 dB. Due to the inclusion of a certain redundancy in selecting the LDPC decoding FER switching threshold, the SNR difference will be slightly greater than zero in turbulence different from the original scheme, indicating a slight delay in switching. In summary, the conventional ACM scheme, when directly transplanted to different turbulence scenarios, leads to waste in bits efficiency or communication interruptions. Moreover, as the difference from the original turbulence increases, these issues are exacerbated. However, the ACM scheme with FER switching standard effectively addresses the transplanted issues of the ACM scheme under different turbulence conditions, with an average cost of around 0.35 dB. This approach aligns better with the rapidly changing atmospheric channels caused by turbulence.

Fig. 8(a) illustrates the specific scenario of weak turbulence (0.5) from Fig. 7. It can be observed that under weak turbulence, the same coding and modulation order exhibit better BER performance. Therefore, directly transplanting the ACM scheme designed for moderate turbulence to weak turbulence leads to a delay in switching process. In other words, it fails to timely switch to a higher coding and modulation index that satisfies the FEC threshold, resulting in waste of bits efficiency. However, with the adoption of FER threshold switching, the sensitivity of the ACM scheme improves by an average of 1.8 dB, enabling an earlier switch in coding and modulation index. This improves bits efficiency to a certain extent while meeting the FEC threshold and enhances the communication rate.

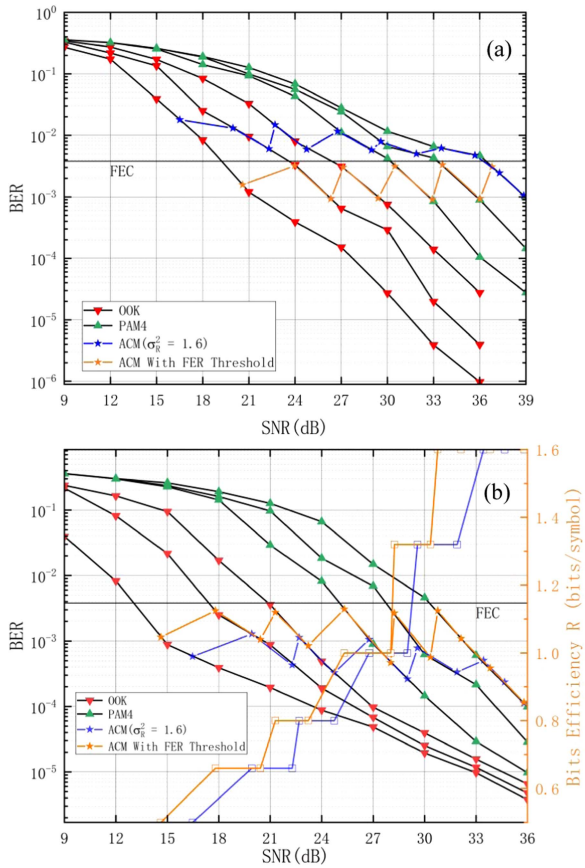

Fig. 8. BER and Bits Efficiency versus SNR with different coding and modulation order under (a) weak turbulence (b) strong turbulence.

Fig. 8(b) depicts the specific scenario of strong turbulence (3.5) from Fig. Similarly, the same coding and modulation format exhibit poorer BER performance under strong turbulence. When directly transplanting the ACM scheme designed for moderate turbulence to strong turbulence, it leads to the issue of switching to a coding and modulation scheme that does not meet the FEC threshold, resulting in communication interruption. However, with the adoption of FER threshold switching, the sensitivity of the ACM scheme improves by an average of approximately 4 dB. The ACM scheme is able to delay the switch and thereby meet the FEC threshold, ensuring regular communication and achieving a relatively ideal communication quality.

The traditional ACM scheme has advantages in bits efficiency compared to fixed coding and modulation order. However, due to the presence of turbulence, the ACM scheme developed for moderate turbulence may result in waste of bits efficiency or communication interruptions when used under different turbulence intensities. In this paper, an ACM scheme with hybrid switching standards is proposed, utilizing LDPC decoding error rate determination at the receiver. This approach enables the ACM scheme to be effectively transplanted to different turbulence intensities at the cost of about 0.35 dB. It enhances communication quality and speed, making it more suitable for atmospheric channels with rapidly changing turbulence conditions.

V. Conclusion

In this paper, an improved ACM scheme with hybrid switching standard is proposed for UAV-to-Ground FSO channels to address the challenges associated with portability across different turbulence conditions, which is validated by simulation. It is observed that the GRU estimator achieves approximately 34.9% improvement in training time compared to the LSTM estimator, without any degradation in system performance. Additionally, a hybrid switching standard based on FER of LDPC decoding is introduced. This standard significantly improves the SNR switching threshold deviation of the ACM scheme from 1.8 dB and 4 dB, which were observed in moderate turbulence conditions, to an average of 0.35 dB. This improvement allows for the effective implementation of the ACM scheme in different turbulence intensities at a relatively small cost, thereby enhancing the communication quality of FSO systems in atmospheric channels characterized by turbulent variations.

The ACM scheme proposed in this paper is implemented based on IM/DD. With some modifications, this system can also be applied to coherent communication. For instance, in PSK modulation, more complex switches between modulation formats, such as QPSK, 8PSK, 16PSK, or even higher-order modulation schemes, can be implemented. Additionally, after optimizing the system to facilitate an increase in DSP speed, there is potential for higher communication bit rates. These advancements will be explored in future research.

References

[1] H. Kaushal and G. Kaddoum, "Optical communication in space: Challenges and mitigation techniques," *IEEE Commun. Surveys Tuts.*, vol. 19, no. 1, pp. 57–96, Firstquarter 2017.

[2] H. Huang, Y. Peng, Y. Lin, W. Fan, Y. Chen, and H. Lu, "5G NR fiber-FSO-wireless systems with dual-polarization and single-carrier optical modulation schemes," *Opt. Commun.*, vol. 530, 2023, Art. no. 129197.

[3] H. Al-Mohammed, M. Al-Ali, and E. Yaacoub, "FSO communication system for high-speed trains under varying visibility conditions," *Veh. Commun.*, vol. 43, 2023, Art. no. 100634.

[4] H. Liang, Y. Li, M. Miao, C. Gao, and X. Li, "Analysis of selection combining hybrid FSO/RF systems considering physical layer security and interference," *Opt. Commun.*, vol. 497, 2021, Art. no. 127146.

[5] R. Lu, J. Wang, X. Fu, S. Lin, Q. Wang, and B. Zhang, "Performance analysis and optimization for UAV-based FSO communication systems," *Phys. Commun.*, vol. 51, 2022, Art. no. 101594.

[6] M. Mohsin and I. A. Murdas, "Performance analysis of an outdoor Li-Fi system-based AO-OFDM architecture under different FSO turbulence and weather conditions," *Optik*, vol. 273, 2023, Art. no. 170427.

[7] B. Dutta, B. Kuiri, R. Atta, N. Sarkar, and A. Patra, "Numerical evaluation of bidirectional high-speed data transmission over turbulence tolerable FSO link employing WDM-OAM multiplexing and DP-QPSK modulation techniques," *Opt. Commun.*, vol. 546, 2023, Art. no. 129753.

[8] M. A. Esmail, "Experimental performance evaluation of weak turbulence channel models for FSO links," *Opt. Commun.*, vol. 486, 2021, Art. no. 126776.

[9] Y. Bian et al., "Low-complexity parallel real-valued weight adaptive digital combining algorithm for coherent FSO communications employing modes diversity reception under atmospheric turbulence channel," *Opt. Commun.*, vol. 474, 2020, Art. no. 126078.

[10] B. K. Saw, V. Janyani, and G. Singh, "Analysis of coherent-OFDM modulation for FSO communication over distribution with pointing errors," *Opt. Commun.*, vol. 545, 2023, Art. no. 129677.

[11] E. Erdogan, I. Altunbas, G. K. Kurt, and H. Yanikomeroglu, "The secrecy comparison of RF and FSO eavesdropping attacks in mixed RF-FSO relay networks," *IEEE Photon. J.*, vol. 14, no. 1, Feb. 2022, Art. no. 7901508.

[12] C.-H. Yeh, Y.-R. Xie, C.-M. Luo, and C.-W. Chow, "Integration of FSO traffic in ring-topology bidirectional fiber access network with fault protection," *IEEE Commun. Lett.*, vol. 24, no. 3, pp. 589–592, Mar. 2020.

[13] R. Samy, H.-C. Yang, T. Rakia, and M.-S. Alouini, "Ergodic capacity analysis of satellite communication systems with SAG-FSO/SH-FSO/RF transmission," *IEEE Photon. J.*, vol. 14, no. 5, Oct. 2022, Art. no. 7347909.

[14] V. Mai and H. Kim, "Beam steering and divergence control using variable focus liquid lenses for WDM FSO communications," *IEEE Photon. Technol. Lett.*, vol. 34, no. 22, pp. 1226–1229, Nov. 2022.

[15] M. J. Saber, J. Mazloum, A. M. Sazdar, A. Keshavarz, and M. J. Piran, "On secure mixed RF-FSO decode-and-forward relaying systems with energy harvesting," *IEEE Syst. J.*, vol. 14, no. 3, pp. 4402–4405, Sep. 2020.

[16] C. Abou-Rjeily, "Packet unloading strategies for buffer-aided multiuser mixed RF/FSO relaying," *IEEE Wireless Commun. Lett.*, vol. 9, no. 7, pp. 1051–1055, Jul. 2020.

[17] R. Li, T. Chen, L. Fan, and A. Dang, "Performance analysis of a multiuser dual-hop amplify-and-forward relay system with FSO/RF links," *J. Opt. Commun. Netw.*, vol. 11, pp. 362–370, 2019.

[18] S. Song, Y. Liu, T. Xu, and L. Guo, "Hybrid FSO/RF system using intelligent power control and link switching," *IEEE Photon. Technol. Lett.*, vol. 33, no. 18, pp. 1018–1021, Sep. 2021.

[19] H. Zhou, S. Mao, and P. Agrawal, "Optical power allocation for adaptive transmissions in wavelength-division multiplexing free space optical networks," *Digit. Commun. Netw.*, vol. 1, pp. 171–180, 2015.

[20] H. Safi, A. A. Sharifi, M. T. Dabiri, I. S. Ansari, and J. Cheng, "Adaptive channel coding and power control for practical FSO communication systems under channel estimation error," *IEEE Trans. Veh. Technol.*, vol. 68, no. 8, pp. 7566–7577, Aug. 2019.

[21] N. D. Chatzidiamantis, A. S. Lioumpas, G. K. Karagiannidis, and S. Arnon, "Adaptive subcarrier PSK intensity modulation in free space optical systems," *IEEE Trans. Commun.*, vol. 59, no. 5, pp. 1368–1377, May 2011.

[22] N. Alshaer, T. Ismail, and M. E. Nasr, "Enhancing earth-to-satellite FSO system spectrum efficiency with adaptive M-ary PSK and SIMO in presence of scintillation and beam wander," *AEU - Int. J. Electron. Commun.*, vol. 125, 2020, Art. no. 153366.

[23] I. B. Djordjevic, "Adaptive modulation and coding for free-space optical channels," *J. Opt. Commun. Netw.*, vol. 2, no. 5, pp. 221–229, May 2010.

[24] Z. Ghassemlooy, W. Popoola, and S. Rajbhandari, "*Optical Wireless Communications System and Channel Modelling with MATLAB*," Boca Raton, FL, USA: CRC Press, 2019.

[25] K. Greff, R. K. Srivastava, J. Koutník, B. R. Steunebrink, and J. Schmidhuber, "LSTM: A search space odyssey," *IEEE Trans. Neural Netw. Learn. Syst.*, vol. 28, no. 10, pp. 2222–2232, Oct. 2017.

[26] Sonali, A. Dixit, and V. K. Jain, "SNR-and rate-optimized LDPC codes for free-space optical channels," *IEEE Access*, vol. 9, pp. 13212–13223, 2021.

[27] Z. Zhong, Y. Huang, Z. Zhang, X. You, and C. Zhang, "A flexible and high parallel permutation network for 5G LDPC decoders," *IEEE Trans. Circuits Syst. II: Exp. Briefs*, vol. 67, no. 12, pp. 3018–3022, Dec. 2020.